Nonlinear optical susceptibilities of disordered aggregates: A comparison of schemes to account for intermolecular interactions

Jasper Knoester
Chemical Physics, University of Groningen, Nijenborgh 4, 9747 AG Groningen, The Netherlands
(Received 28 August 1992)

The performance of approximate theories for the collective nonlinear optical response of assemblies of interacting molecules is investigated by comparing their predictions to exact calculations. To this end, the nonlinear absorption coefficient of linear molecular aggregates with energetic disorder is studied with the aid of Monte Carlo simulations. It is shown that the well-known local-field approximation (LFA) cannot describe the *near-resonance* nonlinear absorption spectrum for disorder values up to the nearest-neighbor intermolecular interactions; surprisingly, it is found that the validity of the LFA does not at all improve with growing disorder. By contrast, the "excitonic two-level system" approximation, in which each collective one-photon transition (Frenkel exciton) of the assembly is treated as an independent two-level system, turns out to describe the collective nonlinear response of the aggregates in a much better way and, moreover, rapidly improves for growing disorder values. It is shown that both models correctly describe the linear optical response and that, within the framework of the LFA, a close connection exists between the rotating-wave approximation and the Heitler-London approximation.

PACS number(s): 36.40.+d, 42.65.−k, 42.50.Fx, 73.20.Dx

I. INTRODUCTION

The calculation of the nonlinear optical response from nanostructures, such as molecular aggregates [1–14], polymers [15–17], and semiconductor microcrystals [18–21] is an important problem because of the interest in their special optical properties. The interactions between the constituents in these systems give rise to collective (delocalized) electronic eigenstates, which in turn lead to collective effects in the optical response. Well-known and rather trivial examples of such effects are shifts in absorption and fluorescence spectra [1,2]. More exciting signatures of collective optical response, however, are (i) exciton superradiance (or cooperative spontaneous emission) [4,5,9–15,18–22], (ii) motional narrowing [1,2,4,14,23], and (iii) "giant" nonlinear optical susceptibilities [8–11,18,24]. Theoretically, the interactions pose the problem of calculating the electronic (excitonic) eigenstates, as these form the basis for the application of standard nonlinear response theory. Even in the case of *linear* optics, where only the limited class of exited states is relevant that can be reached from the ground state by a one-photon transition, this may already be a difficult problem, especially if the system contains disorder [14]. For molecular systems, these *one-particle states* that determine the linear response are the well-known Frenkel excitons [25,26]. The calculation of the optical response, however, becomes almost forbiddingly complicated in the *nonlinear* regime, where multiply exited states (two or more correlated particles) are accessible. In general, these states are impossible to obtain analytically, even for perfectly ordered systems; moreover, the numerical determination of these states is very difficult because of the large matrices that need to be diagonalized (see Sec. II). Therefore the nonlinear optical response of extended systems with interactions is mostly treated with approximate theories. The best known example is the *local-field approximation* (LFA) [27,28]. This is a mean-field approximation [29], in which the interactions are incorporated by adding to the external field that acts on a given particle (excited molecule; electron) a *classical* contribution caused by the polarization of all other particles in the system, without taking into account the quantum correlations that exist between the various particles. Traditionally, the LFA has played an important role in the realm of linear polarization phenomena [30], nowadays, it is also frequently used to describe the nonlinear optical response in condensed phases [24,31]. Very recently, however, the LFA has been seriously criticized following model calculations on homogeneous molecular aggregates which showed that near resonance, local-field theory does not correctly describe the nonlinear absorption coefficient [11,32]. A second approximation consists of assuming that each one-photon transition (probed in linear optics) responds to the external fields as an independent two-level system. The total nonlinear response of the system then simply follows by superimposing the response of these noninteracting two-level systems. This approximation, which can be found in recent literature [13,14,17], is intuitively correct if the various one-photon states are well separated. Its validity has, however, never been studied systematically. Within the framework of molecular assemblies, to which we will restrict ourselves in this paper, we will refer to this approximation as the *excitonic two-level system* (ETLS) model. A third approximation consists of neglecting the interactions altogether. Then, the system's optical response is a superposition of the response of its single constituents and any collective effects are completely missed. This trivial approximation may serve as a zeroth-order point of reference.

Based on the general idea that in the presence of disorder the eigenstates have a tendency to localize on part of

the system [14,33], one may expect that interactions play a less important role with increasing disorder, so that the approximate theories will improve their validity.

The main objective of this paper is to study the performance of the above-mentioned approximate theories by comparing their predictions for the first- and third-order optical response of linear molecular aggregates to exact results. Linear aggregates have received considerable attention lately [1–14]. Moreover, these systems provide an ideal testing ground, as the exact expressions for their nonlinear response are relatively easy to evaluate. In particular, attention is paid to the role of energetic disorder (inhomogeneity), which requires numerical simulations. The organization of this paper is as follows. In Sec. II we discuss the general linear and third-order response of molecular assemblies, without alluding to a specific model or experimental technique. In Sec. II A the exact expressions for the (non)linear susceptibilities are given in terms of the, as yet unknown, one- and two-exciton eigenstates. In Sec. II B we derive and discuss these susceptibilities in the approximate theories (noninteracting molecules, LFA, and ETLS). It is shown that in the case of linear response, the LFA and the ETLS model are equivalent to the exact theory. Next, in Sec. III, we apply the general expressions for the third-order response to disordered linear molecular aggregates, where we focus on the susceptibility that describes nonlinear absorption. Also, we briefly discuss the simulation method in this section. Analytical results for the off-resonance nonlinear absorption at arbitrary magnitude of the disorder and for the resonant nonlinear absorption of homogeneous aggregates are discussed in Sec. IV. In Sec. V we present and discuss the results of our numerical simulations for the resonant nonlinear absorption for chains with diagonal disorder that ranges in magnitude from 0.05 to 1 times the nearest-neighbor intermolecular interaction. Finally, in Sec. VI we summarize our findings. An Appendix contains the technical details of the local-field approximation.

II. OPTICAL RESPONSE OF MOLECULAR ASSEMBLIES: GENERAL THEORY

A. Exact formalism for $\chi^{(1)}$ and $\chi^{(3)}$

In this section, we consider the general theory of (multicolor) frequency-domain optical response of a dilute distribution of molecular assemblies. We will make the following assumptions about the assemblies: (i) They consist of nonpolar molecules that have only one relevant electronic transition, so that they may be considered two-level absorbers. (ii) The size of each assembly is small compared to an optical wavelength. The latter restriction is not essential, but applies to many situations of practical interest. It may be relaxed without major complications, by accounting for the phase differences of the electric fields over the assembly introduced by finite wave vectors [11]. Apart from these restrictions, the system is general. We allow for arbitrary dimensionality and for disorder in the transition frequencies and the positions (interactions) of the molecules that make up an assembly, while also the magnitudes and orientations of the individual molecular transition dipoles within an assembly are not necessarily equal. As the density of assemblies is low, we may neglect the interactions between them, so that the optical response of the total system is obtained from superimposing the response of individual assemblies.

The optical response of one assembly is obtained by applying response theory to the Hamiltonian

$$\hat{H}=\hat{H}_0-\sum_n \hat{\boldsymbol{\mu}}_n\cdot\mathbf{E}(\mathbf{r}_n,t)\ , \tag{1}$$

where $\hat{H}_0$ is the Hamiltonian of the assembly, $\hat{\boldsymbol{\mu}}_n$ is the dipole operator of molecule n, and $\mathbf{E}(\mathbf{r}_n,t)$ denotes the external electric field at position $\mathbf{r}_n$ of molecule n. The electric field is a superposition of a few plane-wave components i, which are characterized by their frequencies $\omega_i>0$, wave vectors $\mathbf{k}_i$, and amplitudes $\mathbf{E}_i$:

$$\begin{aligned}\mathbf{E}(\mathbf{r},t)&=\tfrac{1}{2}\sum_i \mathbf{E}_i\exp(i\mathbf{k}_i\cdot\mathbf{r}-i\omega_i t)+\text{c.c.}\\&=\tfrac{1}{2}\sum_i \mathbf{E}_i\exp(-i\omega_i t)+\text{c.c.}\ ,\end{aligned} \tag{2}$$

where c.c. stands for the complex conjugate and the last step is a consequence of the size restriction that we imposed on the assembly. In this limit, the assembly's optical response is fully determined by its total dipole, which can also be separated in its frequency components:

$$\langle\hat{\mathbf{P}}(t)\rangle\equiv\sum_n\langle\hat{\boldsymbol{\mu}}_n(t)\rangle=\tfrac{1}{2}\sum_i\mathbf{P}_i\exp(-i\omega_i t)+\text{c.c.} \tag{3}$$

Here $\langle\ \rangle$ denotes the quantum-mechanical expectation value. We define the optical susceptibilities of the assembly as the expansion coefficients of the amplitudes $\mathbf{P}_i$ in terms of the electric field amplitudes:

$$\begin{aligned}\mathbf{P}_i=&\chi^{(1)}(-\omega_i;\omega_i)\cdot\mathbf{E}_i+\sum_{j,k}{}^{*}\chi^{(2)}(-\omega_i;\omega_j,\omega_k):\mathbf{E}_j\mathbf{E}_k\\&+\sum_{j,k,l}{}^{*}\chi^{(3)}(-\omega_i;\omega_j,\omega_k,\omega_l)\vdots\mathbf{E}_j\mathbf{E}_k\mathbf{E}_l+\cdots\ ,\end{aligned} \tag{4}$$

where the asterisk on the summations indicates that the sum of the frequencies ω_j, ω_k, etc., must equal ω_i. $\chi^{(i)}$ is a tensor of rank $i+1$, whose second (third, etc.) index is contracted with $\mathbf{E}_j$ ($\mathbf{E}_k$, etc.); if ω_j is replaced $-\omega_j$, $\mathbf{E}_j$ should be replaced by its complex conjugate $\mathbf{E}_j^*$ (analogous for k and l). For our system of nonpolar two-level molecules, $\chi^{(2)}$ vanishes identically. We note that the $\chi^{(i)}$ defined by Eq. (4) are generally referred to as the (hyper)polarizabilities of the assembly; here, we rather use the word "susceptibilities," to distinguish them from the (hyper)polarizabilities of the individual molecules, which also play an important role in this paper. Of course, in an experiment one observes the *macroscopic* susceptibility of the total ensemble of molecular assemblies, which is given by

$$\chi^{(i)}_{\text{mac}}=\eta\langle\chi^{(i)}\rangle_d\ , \tag{5}$$

where η is the density of assemblies and $\langle\ \rangle_d$ denotes an average over any disorder in the system [energetic, positional, and (or) orientational]. The standard ways to calculate the susceptibilities consist of either using nonlinear

response theory [27,28,34] or iteratively solving nonlinear equations of motion [11,35]. Both methods essentially involve the diagonalization of the unperturbed Hamiltonian $\hat{H}_0$. We will only focus on the electronic degrees of freedom and not consider vibrations or phonons. In that case, $\hat{H}_0$ is the Frenkel-exciton Hamiltonian, which in second quantized form and within the Heitler-London approximation reads [25,26]

$$\hat{H}_0=\sum_n \hbar\Omega_n \hat{B}_n^\dagger \hat{B}_n+\sum_{n,m}{}' \hbar V_{nm}\hat{B}_n^\dagger \hat{B}_m \equiv \sum_{n,m}\hbar H_{nm}\hat{B}_n^\dagger \hat{B}_m \ , \tag{6}$$

where $\hat{B}_n$ and $\hat{B}_n^\dagger$ denote the Pauli annihilation and creation operators for an excitation on molecule n, respectively. Ω_n is the transition frequency of molecule n and V_{nm} is the (dipole-dipole) interaction matrix element between the molecules n and m, which tends to delocalize the excitations over the assembly. The prime on the summation excludes the case $n=m$. The Hamiltonian Eq. (6) conserves the number of excitations, so that the eigenstates separate into classes of linear combinations of states with a fixed number of molecules excited: exciton manifolds (see Fig. 1). In order to describe linear response, it is sufficient to know the eigenstates of $\hat{H}_0$ that can be reached from the overall ground state $|0\rangle$ (with all molecules in the ground state) by absorption of one photon. These states are the *one-excitons* (or Frenkel excitons):

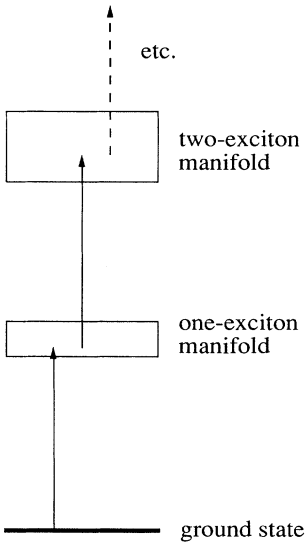

FIG. 1. Schematic representation of the energy levels of an assembly of two-level molecules. The assembly's excited states separate into manifolds (bands) in which the total number of excitations shared by the molecules is a constant. The separation between two consecutive manifolds is on the order of a typical single-molecule transition energy, whereas the width of the n-exciton manifold is on the order of $4n$ times the typical intermolecular interaction. Optical transitions are only allowed between two consecutive manifolds.

$$|\sigma\rangle=\sum_n \varphi_{\sigma n}|n\rangle \ , \tag{7}$$

where $|n\rangle$ denotes the state in which only molecule n is excited, and $\varphi_{\sigma n}$ is the nth component of the normalized σth eigenvector of H_{nm}; the eigenvalue Ω_σ gives the frequency of the exciton $|\sigma\rangle$. Linear response thus involves the diagonalization of an $N\times N$ matrix, where N is the number of molecules in the assembly. To describe higher-order optical processes, we need eigenstates that can be reached from the ground state in two or more optical transitions. The simplest of these, the *two-excitons*

$$|\sigma_1\sigma_2\rangle=\sum_{n_1,n_2}\varphi_{\sigma_1\sigma_2 n_1 n_2}|n_1 n_2\rangle \tag{8}$$

follow from an $N(N-1)/2\times N(N-1)/2$ matrix diagonalization. Here $\sigma_1\sigma_2$ formally represents one label; the two-exciton frequency is denoted $\Omega_{\sigma_1\sigma_2}$. Three-excitons involve a matrix of the order N^3, etc. Thus the difficulty of calculating the higher excited states increases rapidly for typical aggregate sizes.

The transition dipole operator of the total aggregate,

$$\hat{\mathbf{P}}=\sum_n \boldsymbol{\mu}_n(\hat{B}_n^\dagger+\hat{B}_n) \ , \tag{9}$$

has nonzero matrix elements only between two consecutive exciton manifolds. Here, $\boldsymbol{\mu}_n$ is the dipole matrix element of molecule n, which is assumed real. The transition dipole from the ground state to the one-exciton $|\sigma\rangle$ is

$$\boldsymbol{\mu}_{0\sigma}\equiv\langle 0|\hat{\mathbf{P}}|\sigma\rangle=\sum_n \varphi_{\sigma n}\boldsymbol{\mu}_n \ . \tag{10}$$

Similarly, the transition dipoles between the one- and two-exciton manifolds, $\boldsymbol{\mu}_{\sigma,\sigma_1\sigma_2}\equiv\langle\sigma|\hat{\mathbf{P}}|\sigma_1\sigma_2\rangle$, can be expressed in terms of the expansion coefficients $\varphi_{\sigma n}$ and $\varphi_{\sigma_1\sigma_2 n_1 n_2}$. It follows quite generally from the structure of nonlinear response theory that for calculating the third-order polarization, it suffices to know the one- and two-exciton states. Of course, it *is* possible to reach the three-exciton manifold through three interactions with the external field, but these states do not have a transition dipole to the ground state and, therefore, do not contribute to the third-order polarization. Straightforward application of response theory gives the first- and third-order susceptibilities of the assembly; in the rotating-wave approximation (RWA) with respect to all frequencies we find

$$\chi^{(1)}(-\omega;\omega)=-\frac{1}{\hbar}\sum_\sigma \frac{\boldsymbol{\mu}_{0\sigma}\boldsymbol{\mu}_{\sigma 0}}{\omega-\Omega_\sigma+i\Gamma} \tag{11}$$

and

$$\chi^{(3)}(-\omega_s;\omega_1,-\omega_2,\omega_3)=\chi_{\mathrm{I}}^{(3)}(-\omega_s;\omega_1,-\omega_2,\omega_3)+\chi_{\mathrm{II}}^{(3)}(-\omega_s;\omega_1,-\omega_2,\omega_3) \ , \tag{12a}$$

with

$$\chi_{\mathrm{I}}^{(3)}(-\omega_s;\omega_1,-\omega_2,\omega_3)=\frac{2}{8\hbar^3}\sum_{\sigma_1,\sigma_2}\frac{\mu_{0\sigma_1}\mu_{\sigma_1 0}\mu_{0\sigma_2}\mu_{\sigma_2 0}}{(\omega_2-\Omega_{\sigma_2}-i\Gamma)(\omega_s-\Omega_{\sigma_1}+i\Gamma)}\left\{\frac{1}{\omega_1-\Omega_{\sigma_1}+i\Gamma}+\frac{1}{\omega_3-\Omega_{\sigma_2}+i\Gamma}\right\}, \tag{12b}$$

$$\chi_{\mathrm{II}}^{(3)}(-\omega_s;\omega_1,-\omega_2,\omega_3)=-\frac{2}{8\hbar^3}\sum_{\substack{\sigma_1,\sigma_2\\ \sigma_3\sigma_4}}\left\{\frac{\mu_{0\sigma_2}\mu_{\sigma_3\sigma_4,\sigma_1}\mu_{\sigma_2,\sigma_3\sigma_4}\mu_{\sigma_1 0}}{\omega_s-\Omega_{\sigma_2}+i\Gamma}+\frac{\mu_{\sigma_2,\sigma_3\sigma_4}\mu_{\sigma_3\sigma_4,\sigma_1}\mu_{0\sigma_2}\mu_{\sigma_1 0}}{\omega_2-\Omega_{\sigma_2}-i\Gamma}\right\}$$
$$\times\frac{1}{(\omega_3-\Omega_{\sigma_1}+i\Gamma)(\omega_1+\omega_3-\Omega_{\sigma_3\sigma_4}+2i\Gamma)}, \tag{12c}$$

where $\omega_s\equiv\omega_1-\omega_2+\omega_3$. When using Eq. (12) to calculate the assembly's third-order dipole component with frequency ω_s, one should in the spirit of the RWA only allow for the permutations $(\omega_1,-\omega_2,\omega_3)$ and $(\omega_3,-\omega_2,\omega_1)$ of $(\omega_j,\omega_k,\omega_l)$ in Eq. (4). The other permutations contain two antirotating factors. The full expressions for the susceptibilities (i.e., without making the RWA) are obtained from Eqs. (11) and (12) by adding their complex conjugates with opposite frequency arguments: $\omega\rightarrow-\omega$ and $(\omega_s,\omega_1,-\omega_2,\omega_3)\rightarrow(-\omega_s,-\omega_1,\omega_2,-\omega_3)$; moreover, one should then allow for all six permutations of $(\omega_j,\omega_k,\omega_l)$ in Eq. (4). In the derivation of Eqs. (11) and (12), we have invoked a damping model described by the following action on the density operator [32]:

$$\left[\frac{d\hat{\rho}}{dt}\right]_{\mathrm{rel}}=-\Gamma\sum_n(\hat{B}_n^{\dagger}\hat{B}_n\hat{\rho}+\hat{\rho}\hat{B}_n^{\dagger}\hat{B}_n-2\hat{B}_n\hat{\rho}\hat{B}_n^{\dagger}). \tag{13}$$

This describes relaxation of every single-molecule ground-state $\leftrightarrow$ excited-state coherence with rate Γ and of excited-state populations with rate 2Γ; the feeding of the molecular ground state by decay of the excited-state population is described by the last term. Pure dephasing processes are neglected. Within this model, all ground-state $\leftrightarrow$one-exciton coherences in the assembly relax with the same rate Γ; one-exciton populations ($|\sigma\rangle\langle\sigma'|$) and also coherences between the ground state and two-excitons ($|0\rangle\langle\sigma\sigma'|$) all decay with rate 2Γ. Refinement to allow for σ dependence of these damping rates is straightforward in principle. We finally note that the present damping model is not the same as the one found in the superradiant limit [36]; local nonradiative decay channels are assumed to dominate here.

The first contributions to $\chi^{(3)}$ derives from perturbation pathways of the density matrix [34] in which only one-exciton states play a role [Fig. 2(a)]; in the second contribution, also two-exciton states are involved [Fig. 2(b)], which result in the two-exciton resonances in Eq. (12c). A subtle point in the derivation of $\chi^{(3)}$ is the possible feeding of the ground-state population $|0\rangle\langle 0|$ with rate 2Γ from the one-exciton populations $|\sigma_1\rangle\langle\sigma_1|$, which adds the pathways with the dashed arrows in Fig. 2(a). Neglect of this feeding results in unphysical divergencies in $\chi^{(3)}$, as is well known from single-absorber problems [37]. The possible feeding of one-exciton coherences from coherences between one-excitons and two-

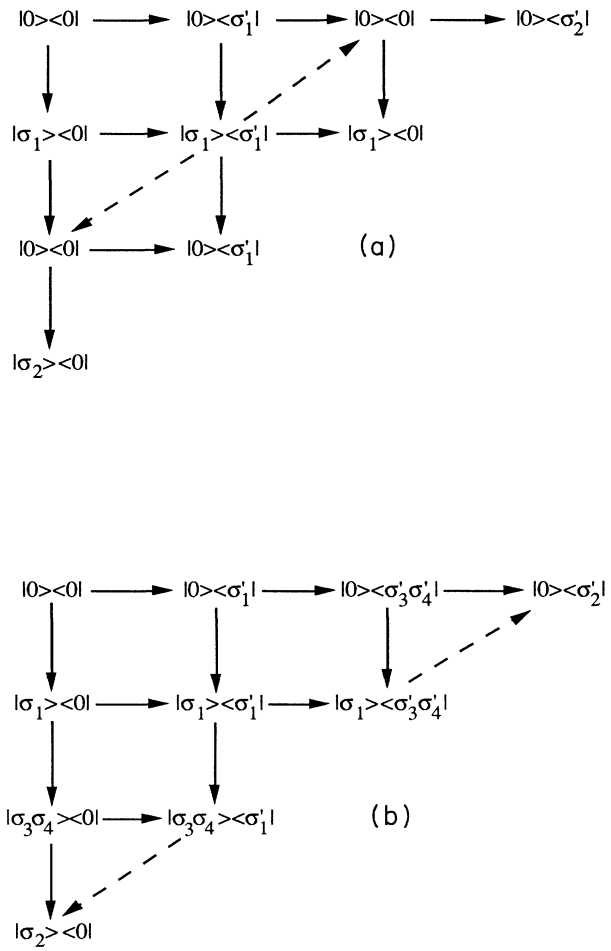

FIG. 2. (a) Diagram representing the Liouville-space pathways that contribute to $\chi_{\mathrm{I}}^{(3)}$ given in Eq. (12b). Every horizontal (vertical) arrow indicates an interaction with one of the external electric fields with the bra (ket) side of the density operator. Each of the eight different pathways that starts from the ground state $|0\rangle\langle 0|$ and follows three (horizontal or vertical) arrows, gives a different contribution to the third-order polarization (see Ref. [34]). Two additional pathways result from the possible feeding of the ground state due to relaxation (with rate 2Γ) of one-exciton populations with $\sigma_1=\sigma_1'$ (dashed arrows). (b) Diagram representing the Liouville-space pathways that contribute to $\chi_{\mathrm{II}}^{(3)}$ given in Eq. (12c). [Cf. (a)].

excitons [dashed arrows in Fig. 2(b)] has been neglected in the calculation of $\chi_{II}^{(3)}$; those processes lead to negligible contributions if Γ is small compared to typical separations between one-exciton levels [38]. Finally, we note that the inclusion of pure dephasing would considerably complicate the calculation of the third-order response, as it would couple all one-exciton populations $|\sigma_1\rangle\langle\sigma_1'|$ to each other in a master equation, and eventually give rise to dephasing-induced extra resonances (see, e.g., Ref. [35]).

Equations (11) and (12) constitute our *exact* results for the linear and third-order response in terms of the one- and two-exciton states, which still depend on the detailed model for the assembly.

B. Approximate theories for $\chi^{(1)}$ and $\chi^{(3)}$

In this section, we introduce three theories for $\chi^{(1)}$ and $\chi^{(3)}$ of a single assembly, which account for the intermolecular interactions (collective eigenstates) in different approximate ways. In the first, "independent-molecule," model, we neglect the interactions completely. In this limiting case, the aggregate's response is just the superposition of the single-molecule responses, so that

$$\chi_{\rm mol}^{(i)}=\sum_n \gamma_n^{(i)} , \tag{14}$$

where $\gamma_n^{(i)}$ denotes the ith-order polarizability of molecule n. We have (in the RWA)

$$\gamma_n^{(1)}(-\omega;\omega)=-\frac{1}{\hbar}\frac{\boldsymbol{\mu}_n\boldsymbol{\mu}_n}{\omega-\Omega_n+i\Gamma} \tag{15a}$$

and

$$\gamma_n^{(3)}(-\omega_s;\omega_1,-\omega_2,\omega_3)=\frac{2}{8\hbar^3}\frac{\boldsymbol{\mu}_n\boldsymbol{\mu}_n\boldsymbol{\mu}_n\boldsymbol{\mu}_n}{(\omega_2-\Omega_n-i\Gamma)(\omega_s-\Omega_n+i\Gamma)}\left\{\frac{1}{\omega_1-\Omega_n+i\Gamma}+\frac{1}{\omega_3-\Omega_n+i\Gamma}\right\} . \tag{15b}$$

These expressions are easily obtained from Eqs. (11) and (12) by restricting the assembly to one molecule, for which the one-exciton states are trivial and the two-exciton states do not exist.

Next, we consider the local-field approximation. In this well-known approximation, the intermolecular interactions within the assembly are incorporated by assuming that each molecule responds to a local field that consists of the external field plus a classical contribution that describes the electric field caused by the other molecular dipoles in the assembly [27–29]:

$$\mathbf{E}_{\rm loc}(\mathbf{r}_n,t)=\mathbf{E}(\mathbf{r}_n,t)-\sum_{m\ (\neq n)}\mathbf{T}(\mathbf{r}_{nm})\cdot\langle\hat{\boldsymbol{\mu}}_m(t)\rangle , \tag{16a}$$

with

$$\mathbf{T}(\mathbf{r})\equiv\frac{r^2\mathbf{1}-3\mathbf{r}\mathbf{r}}{r^5} \tag{16b}$$

the dipole-dipole interaction tensor. The enormous advantage of this approximation is that it simplifies the many-body optical response to a single-molecule response with respect to the *self-consistent field* $\mathbf{E}_{\rm loc}$ (self-consistent, because it depends on the dipoles themselves). Moreover, it turns out that the fulfillment of the self-consistency condition essentially requires the solution of the one-exciton problem only (*vide infra*). It should be realized that the approximate nature of this treatment resides in the fact that in the right-hand side of Eq. (16a) the *expectation values* of the molecular dipoles occur and not the operators themselves; if the operators themselves are kept, Eq. (16a) is of no use, because it is then equivalent to the total Hamiltonian (without the Heitler-London approximation) and requires the solution of the entire many-body problem. Equation (16a) is a mean-field approximation that can be derived quite generally [29] by assuming that the expectation value of any product of operators acting on different molecules can be factorized into the product of the expectation values of the separate operators, e.g.,

$$\langle\hat{\boldsymbol{\mu}}_n(t)\hat{\boldsymbol{\mu}}_m(t)\rangle\rightarrow\langle\hat{\boldsymbol{\mu}}_n(t)\rangle\langle\hat{\boldsymbol{\mu}}_m(t)\rangle . \tag{17}$$

This is only exact if the molecules do not interact, whereas the whole aim of the local-field approximation is to account for interactions. Even without any further calculations, this raises strong doubts concerning this approximation. Equation (16) may alternatively be formulated as

$$\boldsymbol{\mu}_n\cdot\mathbf{E}_{\rm loc}(\mathbf{r}_n,t)=\boldsymbol{\mu}_n\cdot\mathbf{E}(\mathbf{r}_n,t)-\sum_{m(\neq n)}\hbar V_{nm}\langle\hat{B}_m^{\dagger}(t)+\hat{B}_m(t)\rangle , \tag{18}$$

with V_{nm} the interaction matrix element. In this form, the local field is not restricted to dipole-dipole interactions.

The procedure to obtain the susceptibilities now consists of using the self-consistency of the local field in an iterative way [27,39]. First, all the variables are written in terms of a mode expansion like Eq. (3), which defines amplitudes $\langle\hat{\mu}_n\rangle_i$, $\mathbf{E}_{{\rm loc},i}(\mathbf{r}_n)$, etc. By definition, the $\langle\hat{\mu}_n\rangle_i$ can be expanded in terms of the local field at site n through the polarizabilities of molecule n:

$$\langle \hat{\boldsymbol{\mu}}_n \rangle_i = \gamma_n^{(1)}(-\omega_i;\omega_i)\cdot \mathbf{E}_{\mathrm{loc},i}(\mathbf{r}_n) + \sum_{j,k,l}{}^{*} \gamma_n^{(3)}(-\omega_i;\omega_j,\omega_k,\omega_l) \vdots \mathbf{E}_{\mathrm{loc},j}(\mathbf{r}_n) \times \mathbf{E}_{\mathrm{loc},k}(\mathbf{r}_n)\mathbf{E}_{\mathrm{loc},l}(\mathbf{r}_n) + \cdots . \quad (19)$$

This represents a nonlinear set of equations for the $\langle \hat{\boldsymbol{\mu}}_n \rangle_i$ ($n=1,\ldots,N$), which can be solved by reexpansion: we substitute the unknown expansions of the $\langle \hat{\boldsymbol{\mu}}_n \rangle_i$ in terms of the external-field amplitudes $\mathbf{E}_i$ directly into the left-hand side of Eq. (19) and indirectly into the right-hand side by using Eq. (16) or (18) and equate terms of equal powers in the external-field amplitudes that occur on both sides of the equation. This procedure enables us to iteratively solve the expansions for the $\langle \hat{\boldsymbol{\mu}}_n \rangle_i$ in terms of the external-field amplitudes, which, using Eqs. (3) and (4), gives the expressions for the assembly's susceptibilities. The algebra is, in particular for disordered systems with possibly different orientations of the transition dipoles, rather involved and is worked out in detail in the Appendix. Here, we just give the results for $\chi^{(1)}$ and $\chi^{(3)}$, where we restrict to the RWA and for simplicity also confine ourselves to the case where all molecular transition dipoles within the assembly are equal and parallel. We find

$$\chi^{(1)}_{\mathrm{LFA}}(-\omega;\omega) = \sum_n L_n(\omega)\gamma_n^{(1)}(-\omega;\omega) , \quad (20)$$

and

$$\chi^{(3)}_{\mathrm{LFA}}(-\omega_i;\omega_j,\omega_k,\omega_l) = \sum_n L_n(\omega_i)L_n(\omega_j)L_n(\omega_k)L_n(\omega_l) \times \gamma_n^{(3)}(-\omega_i;\omega_j,\omega_k,\omega_l) , \quad (21)$$

with local-field factors

$$L_n(\omega) = \sum_{\sigma,m} \varphi_{\sigma n}\varphi_{\sigma m} \frac{\omega-\Omega_n+i\Gamma}{\omega-\Omega_\sigma+i\Gamma} . \quad (22)$$

If in Eq. (21) ω_j is replaced by $-\omega_j$, $L_n(\omega_j)$ must be replaced by its complex conjugate $[L_n(\omega_j)]^*$ (analogous for k and l). In Eq. (22), the $\varphi_{\sigma n}$ are the one-exciton transformation coefficients, defined in Sec. II A, which have been assumed to be real (the more general form can be found in the Appendix). The general structure of Eqs. (20) and (21) is well known [27,28]: the susceptibilities are given by the single-molecule polarizabilities corrected by local-field factors (one for each frequency that takes part in the process). Equation (22) demonstrates explicitly the above-mentioned fact that one-exciton states are sufficient to account for the self-consistency. *In the LFA, the one-exciton states constitute the only collective input of the assembly into its susceptibilities, no matter the order of the susceptibility.* It is not necessary to determine excitons in higher manifolds. In the usual LFA for bulk systems, this is manifest from the fact that the Lorentz-Lorenz local-field factor $(\epsilon+2)/3$ only depends on the linear dielectric function ϵ. As is clear from Eq. (22), each L_n cancels a molecular resonance in the (hyper)polarizabilities in favor of a collective (one-exciton) resonance. This is physically sound, as the susceptibilities of the assembly should exhibit collective resonances; it is also clear, however, that two-exciton resonances that are contained in the exact expression Eq. (12c) are not recovered in the LFA [11]. In the case of linear optics, where two-excitons play no role, the LFA is exact, as follows quite generally by combining Eqs. (10), (15a), (20), and (22) and comparing the result to Eq. (11). This exactness is also intuitively clear: the factorization approximation Eq. (17) is not relevant for linear optics, as expectation values of two-body operators are at least of second order in the external electric fields. We further note that in the absence of interactions $L_n(\omega)$ reduces to unity, so that the independent-molecule expressions are correctly recovered from Eqs. (20) and (21).

In the general case of arbitrary orientations and magnitudes of the transition dipoles within each assembly, the local-field factors are tensors. Also in this most general situation, which is worked out in the Appendix as well, the only collective knowledge needed to obtain the local-field factors are the one-exciton states, and the linear susceptibility calculated within the LFA is exact. Finally, it is noteworthy that if we do not apply the RWA, the local-field factors are still determined by the one-exciton states, provided that we also relax the Heitler-London approximation (HLA) in the Hamiltonian Eq. (6). Then, too, the LFA is exact for $\chi^{(1)}$. This is shown in the Appendix. It is not surprising that the RWA and the HLA are closely related: In the RWA, one neglects interactions between the positive frequency parts of the dipoles and the electric fields ($\hat{B}_n^{\dagger}\mathbf{E}_i^{*}\exp(i\omega t)$),whereas in the HLA, one neglects the interaction between the positive frequency parts of the dipoles on different molecules ($\hat{B}_n^{\dagger}\hat{B}_m^{\dagger}$) [see Eq. (A19); analogous for the negative frequency parts]. As the LFA mixes the molecule-field and molecule-molecule interactions, it relates the RWA to the HLA.

The third approximation for the assembly's optical response that we discuss here can be found in the literature (see, e.g., Refs. [13,14,17]), but is not known under a specific name. It consists of assuming that each one-photon transition (i.e., ground-state↔one-exciton transition) responds to the external fields as an independent two-level system, which seems justified if the various one-exciton levels are well separated. The total system of N *interacting* two-level molecules is thus replaced by N *noninteracting* two-level systems, with transition frequencies and dipoles of the one-exciton states. Therefore we will refer to this model as the excitonic two-level system model. As in the LFA, the collective optical response is now fully determined by the one-exciton states, irrespective of the order of the nonlinear process. Thus this approximation also misses multiexciton resonances. The first- and third-order susceptibilities follow by using Eqs. (15) for each one-exciton state. For the linear susceptibility, we then recover the exact result Eq. (11), because multiexcitons do not play a role in linear optics. For $\chi^{(3)}$, we obtain

$$\chi^{(3)}_{\rm ETLS}(-\omega_s;\omega_1,-\omega_2,\omega_3)=\frac{2}{8\hbar^3}\sum_{\sigma}\frac{\mu_{0\sigma}\mu_{\sigma 0}\mu_{0\sigma}\mu_{\sigma 0}}{(\omega_2-\Omega_\sigma-i\Gamma)(\omega_s-\Omega_\sigma+i\Gamma)}\left\{\frac{1}{\omega_1-\Omega_\sigma+i\Gamma}+\frac{1}{\omega_3-\Omega_\sigma+i\Gamma}\right\}. \tag{23}$$

III. NONLINEAR ABSORPTION IN LINEAR AGGREGATES

In the preceding section, we did not specify the configuration and the interactions in the molecular assembly. From now on, however we will restrict our study to linear molecular aggregates with nearest-neighbor interactions. Linear systems, such as aggregates and polymers, have received considerable attention lately [1–17]. The prime motivation to restrict to this model, however, is its unique property that all 2^N eigenstates can be found exactly from the diagonalization of only the $N\times N$ matrix H_{nm} [Eq. (6)]: one-excitons, two-excitons, etc. are all determined by diagonalizing this single symmetric tridiagonal matrix [38,40,41]. This enables us to evaluate the exact expressions for the nonlinear response relatively easily, which makes this an ideal model system to assess the validity of the approximate theories. We note that this property holds for arbitrary disorder in the transition frequencies and the interactions on the chain; it only depends on the ordering of the molecules imposed by the linear system in combination with the nearest-neighbor interactions. Furthermore, we stress that no periodic boundary conditions are used. We will assume that all molecular transition dipoles are equal in magnitude (μ) and in orientation (Fig. 3).

The eigenstates are fermion states, which are obtained as follows [38,40,41]. As in Sec. II, let Ω_σ and $\varphi_{\sigma n}$ denote the eigenvalues and normalized eigenvectors of H_{nm}. Then, the N one-exciton states $|\sigma\rangle$ are given by Eq. (7) with energy $\hbar\Omega_\sigma$ and transition dipoles $\boldsymbol{\mu}_{0\sigma}$ from the ground state as in Eq. (10). The expansion coefficients of the multiexciton states [like the $\varphi_{\sigma_1\sigma_2 n_1 n_2}$ in Eq. (8)] are given by Slater determinants of the $\varphi_{\sigma n}$. For instance, the $N(N-1)/2$ independent two-exciton states are now labeled by σ_1 and σ_2 ($\sigma_1>\sigma_2$) and read

$$|\sigma_1\sigma_2\rangle=\sum_{\substack{n_1,n_2\\(n_1<n_2)}}(\varphi_{\sigma_1 n_1}\varphi_{\sigma_2 n_2}-\varphi_{\sigma_1 n_2}\varphi_{\sigma_2 n_1})|n_1 n_2\rangle\ , \tag{24}$$

with energy $\hbar\Omega_{\sigma_1\sigma_2}=\hbar(\Omega_{\sigma_1}+\Omega_{\sigma_2})$, and transition dipoles to the one-exciton manifold

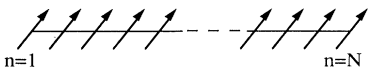

FIG. 3. Linear aggregate of N two-level molecules with parallel transition dipoles, indicated by the arrows, which is introduced as model system in Sec. III.

$$\boldsymbol{\mu}_{\sigma,\sigma_1\sigma_2}=\boldsymbol{\mu}\sum_{\substack{n_1,n_2\\(n_1<n_2)}}(\varphi^*_{\sigma n_1}+\varphi^*_{\sigma n_2})\times(\varphi_{\sigma_1 n_1}\varphi_{\sigma_2 n_2}-\varphi_{\sigma_1 n_2}\varphi_{\sigma_2 n_1})\ . \tag{25}$$

Sum rules for the transition dipoles follow directly from the orthonormality of the eigenvectors $\varphi_{\sigma n}$. Of particular interest are

$$\sum_{\sigma}\boldsymbol{\mu}_{0\sigma}\boldsymbol{\mu}_{\sigma 0}=N\boldsymbol{\mu}\boldsymbol{\mu}\ , \tag{26a}$$

$$\sum_{\substack{\sigma_1,\sigma_2\\(\sigma_1>\sigma_2)}}\boldsymbol{\mu}_{\sigma,\sigma_1\sigma_2}\boldsymbol{\mu}_{\sigma_1\sigma_2,\sigma}=(N-2)\boldsymbol{\mu}\boldsymbol{\mu}+\boldsymbol{\mu}_{0\sigma}\boldsymbol{\mu}_{\sigma 0}\ , \tag{26b}$$

$$\sum_{\substack{\sigma_1,\sigma_2,\sigma_3,\sigma_4\\(\sigma_3>\sigma_4)}}\boldsymbol{\mu}_{0,\sigma_1}\boldsymbol{\mu}_{\sigma_1,\sigma_3\sigma_4}\boldsymbol{\mu}_{\sigma_3\sigma_4,\sigma_2}\boldsymbol{\mu}_{\sigma_2,0}=2N(N-1)\boldsymbol{\mu}\boldsymbol{\mu}\boldsymbol{\mu}\boldsymbol{\mu}\ . \tag{26c}$$

The linear and third-order susceptibilities for the linear aggregate are now obtained by substituting the above frequencies and transition dipoles into the various expressions given in Sec. II. As we have seen quite generally in Sec. II that the linear response is covered exactly by the LFA and in the ETLS model, we will from now on focus on the third-order response of ensembles of aggregates. Specifically, we will study the nonlinear absorption spectrum, which is given by

$$A_{\rm nl}(\omega)=\mathrm{Im}[\langle\langle\mathbf{e}\cdot\chi^{(3)}(-\omega;\omega,-\omega,\omega):\mathbf{eee}\rangle_d\rangle_{\rm ang}]\ , \tag{27}$$

where $\mathbf{e}$ is the unit polarization vector of the incident laser beam and $\omega>0$ is its frequency. Furthermore, $\langle\ \rangle_d$ denotes an average over possible realizations (transition frequencies and intermolecular interactions) of the aggregates and $\langle\ \rangle_{\rm ang}$ is an average over the orientations of the aggregates in the sample. The full nonlinear absorption coefficient contains extra factors, such as the density η of aggregates and the frequency ω [28]. As these factors are equal for all models, they are not of interest in our comparative study and we will omit them here. The orientational average in combination with the tensor nature of $\chi^{(3)}$ ($\sim\boldsymbol{\mu}\boldsymbol{\mu}\boldsymbol{\mu}\boldsymbol{\mu}$) results in a simple prefactor, $\langle(\boldsymbol{\mu}\cdot\mathbf{e})^4\rangle_{\rm ang}\equiv\beta\mu^4$, that is equal for all models. In the results of Secs. IV and V, we will take $\beta=1$, which holds if all aggregates are lined up and $\boldsymbol{\mu}\|\mathbf{e}$. For an isotropic distribution of aggregate orientations, $\beta=\frac{1}{5}$. Henceforth,

we will refer to $A_{\rm nl}(\omega)$ as the nonlinear absorption coefficient. To shorten the notation, we define the detuning from the laser frequency to the σ_ith one-exciton frequency and to the frequency of molecule n as $\Delta_{\sigma_i}\equiv\omega-\Omega_{\sigma_i}$ and $\Delta_n\equiv\omega-\Omega_n$, respectively. The relevant third-order susceptibility is then within the various theories given as follows.

(i) Exact theory [cf. Eqs. (12)].

$$\chi^{(3)}(-\omega;\omega,-\omega,\omega)=\frac{2}{8\hbar^3}\sum_{\sigma_1,\sigma_2}\frac{1}{(\Delta_{\sigma_1}+i\Gamma)(\Delta_{\sigma_2}-i\Gamma)}\left[\boldsymbol{\mu}_{0\sigma_1}\boldsymbol{\mu}_{\sigma_1 0}\boldsymbol{\mu}_{0\sigma_2}\boldsymbol{\mu}_{\sigma_2 0}\left[\frac{1}{\Delta_{\sigma_1}+i\Gamma}+\frac{1}{\Delta_{\sigma_2}+i\Gamma}\right]-\sum_{\substack{\sigma_3,\sigma_4\\(\sigma_3>\sigma_4)}}\boldsymbol{\mu}_{0\sigma_2}\boldsymbol{\mu}_{\sigma_2,\sigma_3\sigma_4}\boldsymbol{\mu}_{\sigma_3\sigma_4,\sigma_1}\boldsymbol{\mu}_{\sigma_1 0}\frac{2\Delta_{\sigma_2}}{(\Delta_{\sigma_3}+\Delta_{\sigma_4}+2i\Gamma)(\Delta_{\sigma_2}+i\Gamma)}\right]. \tag{28}$$

We note that the summations over σ_3 and σ_4 are nested within those over σ_1 and σ_2. Equation (28) has recently been derived by Spano [38,42]

(ii) Independent molecules [cf. Eqs. (14) and (15b)].

$$\chi^{(3)}_{\rm mol}(-\omega;\omega,-\omega,\omega)=\sum_n\gamma^{(3)}_n(-\omega;\omega,-\omega,\omega)=\frac{4}{8\hbar^3}\sum_n\frac{\boldsymbol{\mu}\boldsymbol{\mu}\boldsymbol{\mu}\boldsymbol{\mu}}{(\Delta_n^2+\Gamma^2)(\Delta_n+i\Gamma)}\ . \tag{29}$$

(iii) Local-field approximation [cf. Eqs. (21), (22), and (29)].

$$\chi^{(3)}_{\rm LFA}(-\omega;\omega,-\omega,\omega)=\frac{4\boldsymbol{\mu}\boldsymbol{\mu}\boldsymbol{\mu}\boldsymbol{\mu}}{8\hbar^3}\times\sum_n[K_n(\omega)]^3K_n^*(\omega)(\Delta_n+i\Gamma)\ , \tag{30a}$$

with

$$K_n(\omega)=\sum_{\sigma,m}\varphi_{\sigma n}\varphi_{\sigma m}\frac{1}{\Delta_\sigma+i\Gamma}\ . \tag{30b}$$

(iv) Excitonic two-level systems [cf. Eq. (23)].

$$\chi^{(3)}_{\rm ETLS}(-\omega;\omega,-\omega,\omega)=\frac{4}{8\hbar^3}\sum_\sigma\frac{\boldsymbol{\mu}_{0\sigma}\boldsymbol{\mu}_{\sigma 0}\boldsymbol{\mu}_{0\sigma}\boldsymbol{\mu}_{\sigma 0}}{(\Delta_\sigma^2+\Gamma^2)(\Delta_\sigma+i\Gamma)}\ . \tag{31}$$

We stress that to evaluate any one of the expressions (28)–(31), it suffices to diagonalize the matrix H_{nm}.

From here, only a few further results can be derived by analytical means; this will be done in Sec. IV. In general, numerical techniques are needed, especially if we allow for disorder. The role of disorder is particularly interesting as it tends to localize the exciton eigenstates (the coefficients $\varphi_{\sigma n}$) on part of the chain [14,33]. This may be viewed as a decreasing role of the intermolecular interactions, so that we may expect the approximate theories to improve with growing disorder. We have investigated this for the case of Gaussian diagonal disorder: $\Omega_n=\Omega+D_n$, where D_n is a random energy offset chosen independently for each molecule from a Gaussian distribution with standard deviation D:

$$P(D_n)=\exp(-D_n^2/2D^2)/D\sqrt{2\pi}\ . \tag{32}$$

No interaction disorder was considered; all nearest-neighbor interactions were taken to be $V<0$ (J aggregate). In Sec. V we present the results of this study, which has been conducted by standard Monte Carlo simulation techniques: For every value of D, an ensemble of aggregates was randomly generated, the matrix H_{nm} for each aggregate was diagonalized, and its contribution to the nonlinear absorption coefficient calculated according to Eqs. (27)–(31). Statistical errors in the ensemble-averaged absorption coefficients were estimated by splitting the total ensemble into ten subensembles and calculating the standard deviation of the ten subaverages. The number of aggregates within the total ensemble was chosen such that the statistical errors were small enough to make the comparison between the various theories significant (see Sec. V). All calculations were performed on a Convex C230 computer, with the use of vectorized NAG library routines [43].

IV. OFF-RESONANCE RESPONSE AND HOMOGENEOUS AGGREGATES

In this section, we discuss two regimes that can be handled by analytical means. The first is the off-resonance form of $\chi^{(3)}(-\omega;\omega,-\omega,\omega)$. Let $\Delta\equiv\omega-\Omega$ denote the detuning of the laser frequency from the average molecular transition frequency and let us assume that we are far away from all resonances: $|\Delta|\gg V|,D,\Gamma$. (However, $|\Delta|$ is still small enough to justify the RWA.) We then have $\Delta_\sigma\approx\Delta_n\approx\Delta$ (all σ and n). Substituting this into Eq. (28) and using the sum rules (26a) and (26c), we find

$$\chi^{(3)}(-\omega;\omega,-\omega,\omega)\approx N\frac{4}{8\hbar^3}\frac{\boldsymbol{\mu}\boldsymbol{\mu}\boldsymbol{\mu}\boldsymbol{\mu}}{(\Delta^2+\Gamma^2)(\Delta+i\Gamma)}\ . \tag{33}$$

Note the proportionality to N, even though the one-exciton ($\chi^{(3)}_{\rm I}$) and two-exciton ($\chi^{(3)}_{\rm II}$) contributions separately scale like N^2; a delicate cancellation occurs between these two terms [9–11]. From Eqs. (29) and (30) it is easily found that the same off-resonance expressions hold for the independent-molecule model and in the LFA. It should be stressed that this holds for every ag-

gregate separately and is not a consequence of the disorder average. By contrast, the ETLS model [Eq. (31)] does not give the correct off-resonance behavior: the factor $N\mu^4$ in Eq. (33) should for this model by replaced by $\sum_\sigma |\mu_{0\sigma}|^4$, which varies between $N\mu^4$ in the limit of very strong disorder ($D \gg |V|$) and $\alpha N^2\mu^4$ in the case of vanishing disorder (α is a constant of the order unity). The delicate cancellation between one- and two-exciton contributions can, of course, no longer occur in this model.

We now turn to the more interesting resonance region, for which analytical results can only be obtained in the case of homogeneous aggregates: $D=0$, or $\Omega_n \equiv \Omega$ for all n, with nearest-neighbor interactions V. We will discuss this in some detail, because it serves as a general reference case when studying disordered aggregates. H_{nm} is now diagonalized by

$$\varphi_{kn} = \left[\frac{2}{N+1}\right]^{1/2} \sin\left[\frac{\pi k n}{N+1}\right], \tag{34a}$$

with eigenfrequencies

$$\Omega_k = \Omega + 2V\cos\left[\frac{\pi k}{N+1}\right], \tag{34b}$$

and wave numbers $k=1,2,\ldots,N$. The eigenvectors φ_{kn} are standing waves which are delocalized over the entire chain. The important transition dipoles are

$$\boldsymbol{\mu}_{0k} = \boldsymbol{\mu}\left[\frac{2}{N+1}\right]^{1/2} \frac{1-(-)^k}{2}\cot(\kappa), \tag{35a}$$

and, after some tedious but straightforward trigonometric algebra,

$$\begin{aligned}\boldsymbol{\mu}_{k,k_1k_2} = \boldsymbol{\mu}\left[\frac{2}{N+1}\right]^{1/2} \Bigg[& \delta_{k,k_2}\frac{1+(-)^{k_1}}{2}\cot(\kappa_1) - \delta_{k,k_1}\frac{1+(-)^{k_2}}{2}\cot(\kappa_2) \\ & + \tfrac{1}{2}\{\delta_{k_1-k_2-k,0} - \delta_{k_1-k_2+k,0}\}[\cot(\kappa_1)+\cot(\kappa_2)] \\ & + \tfrac{1}{2}\{\delta_{k_1+k_2+k,2(N+1)} - \delta_{k_1+k_2-k,0}\}[\cot(\kappa_1)-\cot(\kappa_2)]\Bigg],\end{aligned} \tag{35b}$$

where $\kappa_{(i)} \equiv \pi k_{(i)}/2(N+1)$. From Eqs. (35) and the sum rules (26), it is found that the $|k=1\rangle$ one-exciton state contains almost the entire oscillator strength (dipole squared) from the one-exciton manifold to the ground state [$0.81(N+1)\mu^2$ for $N \gg 1$]. This well-known fact is responsible for exciton superradiance [4,14]. Among the allowed transitions from the $|k=1\rangle$ one-exciton state to the two-exciton manifold, the transition to the $|k_1=2,k_2=1\rangle$ state is dominant, with an oscillator strength of $1.27(N+1)\mu^2$ (70% of the total) for $N \gg 1$. Consequently, in the absence of other damping mechanisms, the $|k_1=2,k_2=1\rangle$ state will superradiate into the one-exciton manifold.

Substituting the above expressions for the eigenfrequencies and the transition dipoles into Eqs. (28)–(31), the nonlinear absorption coefficients for homogeneous aggregates can directly be plotted. In Figs. 4(a) and 4(b), the results are given for a J aggregate of 40 molecules with a damping rate of $\Gamma=0.01|V|$ in the frequency region close to the resonance $\Omega_{k=1}$. The comparison between the exact theory and the LFA [Fig. 4(a)], reveals the same features that have already been discovered by Spano and Mukamel for the case of homogeneous cyclic aggregates [11]. We will briefly highlight the most important points and add some discussion. The exact theory shows a strong bleaching of the $k=1$ one-exciton transition (negative contribution to the absorption), whereas positive contributions to the absorption derive from two-photon absorption (TPA), which is caused by transitions from the ground state via the one-exciton manifold into the two-exciton manifold. TPA is resonant at $2\omega = \Omega_k + \Omega_{k'}$, with $k+k'$ odd. (The TPA in Fig. 4 is mainly due to $k=1, k'=2$). The magnitude of the one-exciton bleaching scales as N^2, because the relevant dipoles scale like $\sqrt{N}$. This scaling marks cooperative ("giant") on-resonance third-order response. We reiterate that off resonance this collectivity is lost [Eq. (33)]. Also, it has been shown that the on-resonance N^2 scaling is strictly limited to aggregate sizes smaller than an optical wave-length; [9,11]; a similar size restriction exists for the superradiant behavior of exciton states [5,22].

The nonlinear absorption spectrum according to the LFA does not at all resemble the exact spectrum. Its shape is strongly dispersive, for which we do not have an intuitive physical explanation. With regard to this point, it should be realized that *the LFA prescribes a scheme to calculate nonlinear response, but it does not explicitly make approximations for eigenstates and (or) eigenfrequencies.* In contrast to the other theories discussed here, it is therefore impossible to point out physical states that cause the observed bleaching and extra absorption effects in the LFA. We further note that the peaks in the LFA scale like N [it is essentially a sum over contributions from separate molecules, see Eq. (30a)]. Nevertheless, the LFA has higher peak values than the exact theory [Fig. 4(a)]. This can be explained from the fact that in Eq. (30a), four resonant denominators may coincide, whereas the exact result only has a triple resonance at $\omega=\Omega_{k=1}$.

In contrast to the LFA, the ETLS model does make direct assumptions about the states in the system and its nonlinear absorption spectrum can be understood much better. The bleaching peak is reasonably well reproduced

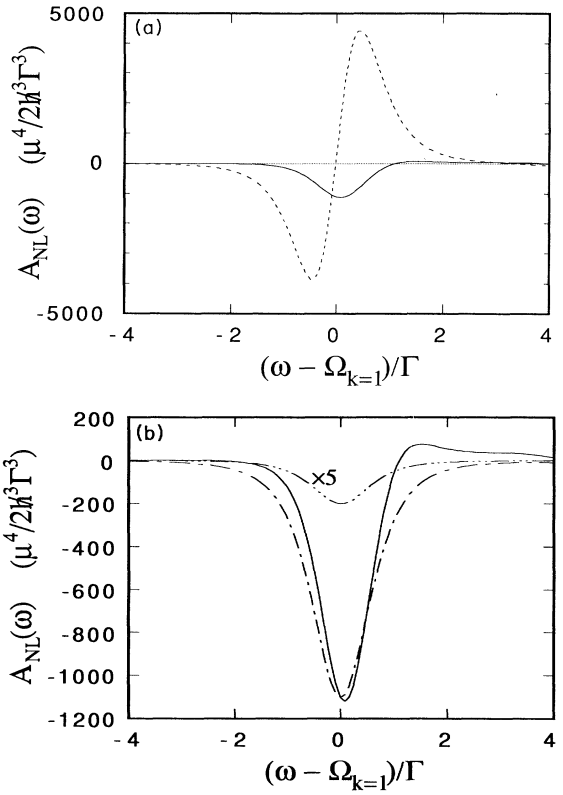

FIG. 4. (a) Nonlinear absorption spectrum for homogeneous linear J aggregates of $N=40$ molecules with $\Gamma=0.01|V|$. $\Omega_{k=1}$ denotes the frequency of the homogeneous $k=1$ one-exciton. The solid line (——) gives the exact result and the dashed curve (— — —) represents the local-field approximation. (b) As in (a); ——: exact result; — - —: excitonic two-level system approximation; and – · · · –: independent molecules. Note that the latter spectrum has been multiplied by a factor of 5 and is redshifted over $\Omega-\Omega_{k=1}$ in order to make it visible.

by this model, whereas the TPA is, of course, completely missed [Fig. 4(b)]. As the TPA peak only has a relatively small spectral content (it has a single resonance only), the overall impression of the ETLS model is reasonably good. The deviations in the bleaching peak from the exact solution result from the neglect of processes in which two different one-excitons play a role [$\sigma_1 \neq \sigma_2$ in the first term of Eq. (28)]; as long as the separations between the one-exciton levels are large compared to Γ, these contributions are small. In the ETLS model, the bleaching maximum correctly scales as N^2. Finally, the independent-molecule model, of course, only exhibits bleaching. This spectrum has the simple form

$$A_{\mathrm{nl,mol}}(\omega) = -\frac{4\mu^4}{8\hbar^3} N \frac{\Gamma}{(\Delta^2+\Gamma^2)^2} , \tag{36}$$

which scales like N for all frequencies and, as the exact spectrum, has a full width at half maximum (FWHM) of approximately 1.29Γ. In Fig. 4(b), this spectrum has been shifted over $\Omega_{k=1}-\Omega$; this shift is also applied in the figures discussed in the next section. In contrast to all other models, the independent-molecule model cannot reproduce the spectral shift associated with the interactions.

V. NUMERICAL SIMULATIONS: RESULTS AND DISCUSSION

In this section we present and discuss the results of our numerical simulations of the nonlinear absorption spectrum for molecular chains with Gaussian diagonal disorder [Eq. (32)]. All simulations were performed on J aggregates ($V<0$) of 40 molecules with a damping rate $\Gamma=0.01|V|$. In Fig. 5 the nonlinear absorption spectra according to the exact and approximate theories are shown for very low disorder: $D=0.05|V|$. The average was obtained from a total ensemble of 25 000 aggregate realizations; the statistical errors in the data are in the order of 2–5%. For this low value of the disorder, the main features of the spectrum are still well understood from perturbative arguments with respect to the disorder contribution in the Hamiltonian, $\hbar\sum_n D_n \hat{B}^\dagger_n \hat{B}_n$. In lowest order, we use the zeroth order, completely delocalized, eigenstates of the homogeneous aggregate [i.e., the φ_{kn} of Eq. (34a)] and the eigenfrequencies to first order in the disorder. The perturbative eigenfrequencies $(\Omega'_{k=1}, \Omega'_{k=2}, \ldots, \Omega'_{k=N})$ have a joint stochastic distribution imposed by the disorder in the molecular frequencies. The disorder-averaged spectra are now obtained by convoluting the homogeneous forms of the spectra with this joint distribution. It can easily be shown that to first order in the Gaussian diagonal disorder, the distribution of every *single* eigenfrequency Ω'_k (irrespective of all other eigenfrequencies) in the linear aggregate is a Gaussian with mean Ω_k and a k-independent FWHM of $W_N \equiv (8\ln 2)^{1/2}[3/2(N+1)]^{1/2}D$ [for circular aggregates one finds $(8\ln 2)^{1/2}D/\sqrt{N}$] [23]. For the linear absorption spectrum, $\mathrm{Im}\langle\chi^{(1)}(-\omega;\omega)\rangle_d$, which is a sum over

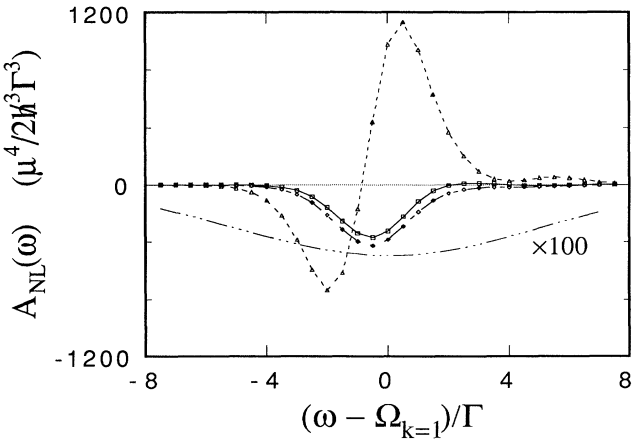

FIG. 5. Simulated nonlinear absorption spectra for J aggregates of 40 molecules with $\Gamma=0.01|V|$ and Gaussian diagonal disorder of magnitude $D=0.05|V|$, according to the various models discussed in the text. Curves are labeled as in Figs. 4(a) and 4(b). The markers indicate the individual data points obtained in the simulation.

single one-exciton contributions [cf. Eq. (11)], this directly implies a FWHM that is considerably lower than the value $(8\ln 2)^{1/2}D \approx 2.35D$ that holds for the independent-molecule spectrum. This phenomenon is known as motional narrowing or exchange narrowing: the intermolecular interactions cause a dramatic narrowing of the linear absorption spectrum, as is, e.g., clearly observed for J aggregates [1,2]. For nonlinear spectra, the situation is more complicated, because the perturbed eigenenergies of different quantum number are mutually correlated, as they all derive from a common underlying molecular disorder. This correlation plays an important role in, e.g., the TPA peaks, which necessarily involve two different eigenfrequencies: $\omega_{\mathrm{TPA}}=(\Omega'_k+\Omega'_{k'})/2$. If all Ω'_k would be distributed independently of each other, every TPA peak would be a Gaussian function centered at $(\Omega_k+\Omega_{k'})/2$, with a FWHM of $W_N/\sqrt{2}$. An approximate analysis (for $N \gg 1$) that does account for the stochastic correlations between the two perturbed eigenfrequencies gives a slightly larger, but still narrowed, value for this FWHM, namely $(8\ln 2)^{1/2}[5/4(N+1)]^{1/2}D$. In contrast to the TPA peak, the much larger exciton bleaching peak is mainly determined by only one eigenfrequency, and is thus well described in terms of the usual motional narrowing picture. This is clearly visible in Fig. 5: The bleaching peak is broader than in the case of the homogeneous aggregate (Fig. 4), but it is not nearly as broad as the independent-molecule spectrum (which is almost Gaussian with a FWHM of $2.35D$). We now define a delocalization range (coherence size) for the exciton states by

$$N_{\mathrm{del}} \equiv \frac{3}{2}\left[\frac{2.35D}{W}\right]^2 - 1 , \tag{37}$$

where W is the FWHM of the bleaching feature in the exact spectrum. Based on this, we find $N_{\mathrm{del}} \approx 32$, which clearly demonstrates that the eigenstates are indeed strongly delocalized over the chain at this low disorder value. We have confirmed this further by calculating the inverse participation ratio (or degree of localization) [14,44], which gives a delocalization range of approximately 30 molecules. It should be noted that the narrowed $(k=1,k'=2)$ TPA is hardly visible anymore: it is almost completely canceled by the distribution of much larger bleaching features. We further observe that the exact spectrum, as well as the other ones, are redshifted relative to the homogeneous spectrum; this disorder-induced redshift is a well-known phenomenon [14,44], which can be understood from the second-order perturbative energy of the $k=1$ exciton state. Figure 5 clearly shows that the ETLS model has improved relative to the homogeneous case. Its shape now closely resembles the exact solution and at the peak the difference in absorption is 15%. By contrast, the LFA did not improve its performance. Its shape is still strongly dispersive, although it has obtained a clear asymmetry and predicts a net absorption in this frequency region, where the other theories give a net bleaching. The small feature in the LFA at $\omega-\Omega_{k=1} \approx 5.5\Gamma$ is due to the $k=3$ one-exciton state.

In Fig. 6 we show the results for $D=0.1|V|$, also obtained from an ensemble of 25 000 aggregates. The statistical errors are smaller than 5% in the main features, except for the LFA, where the errors are roughly 10% in the main feature and increase to 30% in the far wings. Maintaining high accuracy in the simulation of the LFA gets increasingly difficult for higher values of D/Γ. The reason is that in the disorder average a large number of dispersive features with width $\sim\Gamma$ and scattered over a frequency range of the order D cancel each other to a large extent. Consequently, the average spectrum in the LFA requires sampling small differences of large numbers. This makes the simulation of the LFA more difficult than the exact theory, even though for the latter more elaborate and nested summations are needed. Also for $D=0.1|V|$, we observe a clear motional narrowing effect, with $N_{\mathrm{del}} \approx 27$. Furthermore, the redshifts have increased relative to Fig. 5 and the TPA is completely invisible now. The performance of the ETLS model is comparable to the case $D=0.05|V|$: its peak value now deviates from the exact solution by 20%. Relative to Fig. 5, the LFA has obtained an even more pronounced asymmetry towards net absorption.

Figures 7 and 8 show the results for $D=0.5|V|$ and $|V|$, respectively. The ensembles contained 50 000 aggregates, except for the LFA, where separate simulations were done on 1 000 000 and 2 000 000 aggregates. The reason is the slow statistical convergence of the LFA average discussed above. This problem makes straightforward simulations of the LFA in the region $D>|V|$ impossible in practice. The statistical errors are of the same order as for $D=0.1|V|$. If we compare the exact spectra in Figs. 7 and 8 with the independent-molecule results, we observe that motional narrowing is weakened considerably, because the excitons undergo stronger localization due to the disorder [14,33]. Based on the widths of the spectra, we find $N_{\mathrm{del}} \approx 10$ for $D=0.5|V|$ and $N_{\mathrm{del}} \approx 6$ for $D=|V|$ (the inverse participation ratio gives a delocalization range of roughly four molecules in the latter case). We note that, as is observed for linear absorption spectra [14,44], the exact line shape maintains a Gaussian charac-

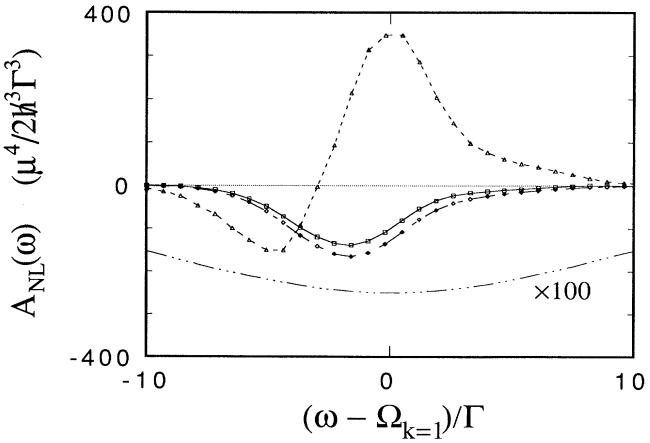

FIG. 6. As Fig. 5, with $D=0.1|V|$.

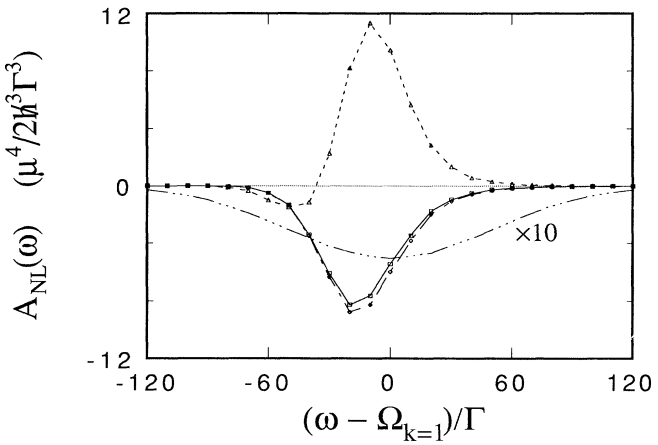

FIG. 7. As Fig. 5, with $D=0.5|V|$.

ter on the red side of the peak, whereas it becomes Lorentzian on the blue (intraband) side. This effect grows as the disorder grows and results, within a (oversimplified) perturbative view, from mixing of the homogeneous k states, which causes the $k\neq 1$ one-excitons to "steal" oscillator strength from the superradiant $k=1$ one-exciton (the bottom of the one-exciton band for $V<0$). In Figs. 7 and 8 it is clearly seen that the ETLS model approaches the exact solution; the peak differences are no more than 6% and 4%, respectively. This rapid approach of the ETLS model towards the exact theory can be understood from the localization of the transformation coefficients $\varphi_{\sigma n}$ on small parts of the chain, with a length that is near the absorption peak characterized by $N_{\rm del}$. The smaller $N_{\rm del}$ gets, the smaller the chance will be that two eigenvectors σ_1 and σ_2 with energies in the region of the lower exciton band edge have appreciable amplitude on the same part of the chain. It then follows immediately from Eq. (24) that

$$|\sigma_1\sigma_2\rangle \rightarrow \pm|\sigma_1\rangle\otimes|\sigma_2\rangle \ , \tag{38}$$

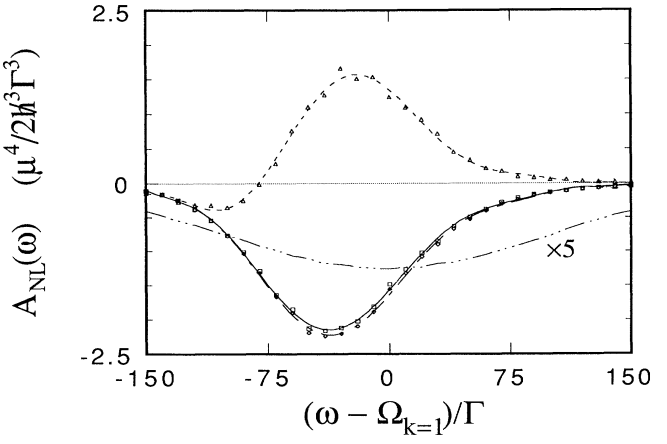

FIG. 8. As Fig. 5, with $D=1.0|V|$.

where the choice of sign depends on the relative position (right or left) of the two eigenvectors on the chain and is, of course, physically irrelevant. Thus the two-excitons that contribute to the absorption (those in the region of the absorption band) are direct products of two one-excitons, so that their nonlinear response is by definition captured within the ETLS model. We note that the argument leading to Eq. (38) holds long before the eigenstates are completely localized on single molecules (which does not happen until $D \gg |V|$), so that the ETLS offers a *non-trivial* way to account for interactions in nonlinear response. This is also obvious from Figs. 7 and 8: the independent-molecule model does not at all capture the line shape and the magnitude of the nonlinear absorption at $D \leq |V|$; collective effects are still important in this disorder region. Finally, we observe that also for $D=0.5|V|$ and $|V|$, the LFA does not approach the exact solution. Even though the absolute magnitude of the peak value is now in the order of the exact solution, the sign is opposite: net absorption versus net bleaching.

VI. SUMMARY AND CONCLUDING REMARKS

In this paper we have investigated the performance of three approximate schemes to account for intermolecular interactions in the nonlinear optical response of molecular assemblies. We have done this by comparing the approximate and exact nonlinear absorption spectra of linear molecular aggregates. Special attention has been paid to the role of energetic disorder, because disorder tends to lessen the importance of interactions, so that the approximations may *a priori* be expected to improve with growing disorder.

The independent-molecule approximation, in which interactions are completely neglected, misses all collective effects of the optical response. It has mainly been introduced as a zeroth-order reference point and to demonstrate motional narrowing effects in the other theories.

The second approximation that we have evaluated is the well-known local-field approximation, in which the assembly's optical susceptibilities are given by the molecular (hyper)polarizabilities, multiplied by local-field factors. It is shown quite generally in this paper that the evaluation of the local-field factors only involves the relatively easy calculation of the assembly's one-exciton eigenstates; knowledge of the multiexciton states is not required in this approximation. The linear response predicted by the LFA is exact for all frequencies, while also the *off-resonance* nonlinear response is correctly described. The latter point is related to the fact that the LFA is very useful to account for the effect of a background index of refraction. However, the LFA fails completely in describing the *on-resonance* nonlinear absorption. For homogeneous (cyclic) aggregates, this had been noted in the literature already [11]; the surprising result of the present study is that the performance of the LFA does *not at all* improve in the presence of energetic disorder (D) ranging up to the nearest-neighbor intermolecular interactions (V). Because the LFA does not make direct assumptions about the eigenstates of the assembly, it is very hard to give a physical explanation for its poor per-

formance. Recently, Cnossen, Drabe, and Wiersma [31] have shown that the LFA explains the second-harmonic generation (SHG) of Langmuir-Blodgett monolayers very well. They suggested that the reason for this success was the presence of strong disorder in their system. Unfortunately, it is impossible to study the LFA in the large-disorder region ($D \gg |V|$) by straightforward numerical simulations, like we used in this paper, because of slow statistical convergence. Based on the trend in our nonlinear absorption spectra with increasing disorder, however, we do not expect that the LFA approaches the exact result until the response is completely dominated by single-molecule effects and the local-field factors have become trivial (unity, in case the background index of refraction is neglected). Instead, we believe that the success of the LFA in treating SHG is related to the fact that in this technique the susceptibility that determines the signal, $\chi^{(2)}(-2\omega;\omega,\omega)$, has a single resonance only (the laser frequency is off resonance, while twice the laser frequency is close to resonance), whereas the nonlinear absorption coefficient has a strong triple resonance. Our model system does not allow for SHG, but calculations of its third-harmonic generation, where three times the laser frequency is taken close to resonance ($3\omega \approx \Omega$), show that the LFA is close to exact for this technique [45]. Therefore our more general conclusion is that the LFA correctly describes experiments that have single resonances with the one-exciton band (note that linear optics is included in this class), but fails at describing multiple resonances or resonances with higher exciton manifolds.

In the excitonic two-level system model, the response of the N interacting molecules in the assembly is approximated by the response of N noninteracting two-level systems with frequencies and dipoles characterized by the assembly's one-exciton transitions. Like the LFA, this approximation only requires knowledge of the one-exciton states and it correctly predicts the linear response; in general, however, it does not recover the exact off-resonance nonlinear response. More importantly, our calculations clearly show that this approximation may very well describe the nonlinear response near multiple resonances. In general, one should expect that the ETLS model is accurate on resonance if the typical separation between one-exciton levels is large compared to their broadening Γ. For homogeneous aggregates, this limits the aggregate size for which this model is useful, as the exciton levels get denser for growing N. For instance, the minimum separation between two allowed transitions on a homogeneous chain is given by $\delta \equiv \Omega_{k=3} - \Omega_{k=1} \approx 8\pi^2 |V|/N^2$ for $N \gg 1$. For disordered aggregates, however, it is more appropriate to use the effective separation $\delta_{\text{eff}} \approx 8\pi^2 |V|/N_{\text{del}}^2$, with $N_{\text{del}} < N$ the exciton delocalization range, so that the ETLS model is in practice much less limited by the aggregate size. Our simulations clearly show that with growing disorder the ETLS nonlinear absorption spectrum rapidly approaches the exact spectrum; this happens long before the disorder is high enough to effectively isolate the molecules from each other and can entirely be understood from the localization of the one-exciton states on segments of the chain. As a further illustration, we notice that the above arguments *a posteriori* justify the use of a simple two-level model (i.e., the ETLS model) to interpret the ratio of fluorescence and Raman yields from J aggregates of pseudo-isocyanine [13]. For these aggregates $N_{\text{del}} \approx 50$ and $|V| \approx 600$ cm^{-1} [14], giving a δ_{eff} in the order of 10 cm^{-1}, which is indeed much larger than the broadening imposed by the exciton lifetime of 70 ps. We conclude that the ETLS model in practice offers a useful way to describe multiply resonant nonlinear optical response of molecular assemblies.

We finally note that from Figs. 4–8 it is seen that the resonant nonlinear optical response of aggregates rapidly decreases with growing disorder. The interesting problem of the scaling of the nonlinear optical response with the aggregate size (N) in the presence of disorder is analyzed in another paper [45].

ACKNOWLEDGMENTS

It is a pleasure to thank Frank C. Spano and Douwe A. Wiersma for helpful discussions. Financial support by the Netherlands Organization for Scientific Research (NWO) is gratefully acknowledged.

APPENDIX: DERIVATION OF THE LOCAL-FIELD FACTORS

In this appendix we derive the local-field expressions for the first- and third-order susceptibilities of general molecular assemblies. The starting point is Eq. (19) of the main text, in which we expanded the expectation value of each molecular dipole in terms of the self-consistent local field. We rewrite the ith amplitude of the molecular transition dipoles as

$$\langle \hat{\boldsymbol{\mu}}_n \rangle_i = \boldsymbol{\mu}_n p_{ni} \ , \tag{A1a}$$

where p_{ni} is the amplitude of the component of

$$p_n(t) \equiv \langle \hat{B}^{\dagger}_n(t) + \hat{B}_n(t) \rangle \tag{A1b}$$

that oscillates with frequency ω_i [compare Eq. (3)]. In terms of these variables, the amplitudes of the assembly's total dipole are

$$\mathbf{P}_i = \sum_n \boldsymbol{\mu}_n p_{ni} \ . \tag{A2}$$

The advantage of writing the variables like this is that the vector nature is separated from the dynamic quantity p_{ni}. We substitute Eq. (A1a) into Eqs. (19) and (16a) and assume that each p_{ni} can be expanded in terms of the *external* field amplitudes, as is done in Eq. (4) for the total dipole. This expansion is now solved iteratively by equating terms of the same order in the external fields that occur in the left- and right-hand sides of Eq. (19). The first-order terms yield as equation

$$\boldsymbol{\mu}_n p_{ni}^{(1)} = \gamma_n^{(1)}(-\omega_i;\omega_i) \cdot \left[\mathbf{E}_i - \sum_{m(\neq n)} \mathbf{T}(\mathbf{r}_{nm}) \cdot \boldsymbol{\mu}_m p_{mi}^{(1)} \right] , \tag{A3}$$

where $p_{mi}^{(1)}$ denotes the first-order contribution to p_{mi}. We rewrite the linear molecular polarizability to separate the

tensor nature

$$\gamma_n^{(1)}(-\omega;\omega)=\frac{\boldsymbol{\mu}_n\boldsymbol{\mu}_n}{\hbar D_n(\omega)} , \tag{A4}$$

so that Eq. (A3) can be recast into the form

$$\sum_m M_{nm}(\omega_i)p_{mi}^{(1)}=\frac{\boldsymbol{\mu}_n\cdot\mathbf{E}_i}{\hbar} . \tag{A5}$$

This represents an inhomogeneous set of N coupled linear equations with the electric field as source. The symmetric $N\times N$ matrix $\mathbf{M}(\omega)$ is defined through

$$M_{nm}(\omega)=D_n(\omega)\delta_{nm}+V_{nm}(1-\delta_{nm}) , \tag{A6a}$$

with

$$\hbar V_{nm}=\boldsymbol{\mu}_n\cdot\mathbf{T}(\mathbf{r}_{nm})\cdot\boldsymbol{\mu}_m , \tag{A6b}$$

the matrix element of the dipole-dipole interaction between molecule m and n. It is noteworthy that Eq. (A6a) is not restricted to dipolar interactions; it may be derived for arbitrary interactions by using an equation-of-motion approach in which factorizations like Eq. (17) are inferred for products of two-molecule operators. Now suppose that we know the eigenvalues, $\Lambda_\sigma(\omega)$, and normalized eigenvectors, $\xi_{\sigma n}(\omega)$, of the matrix $\mathbf{M}(\omega)$. Equation (A5) is then easily solved as

$$p_{mi}^{(1)}=\sum_{\sigma,n}\frac{\xi_{\sigma m}(\omega_i)\xi_{\sigma n}^*(\omega_i)}{\hbar\Lambda_\sigma(\omega_i)}\boldsymbol{\mu}_n\cdot\mathbf{E}_i . \tag{A7}$$

Substituting Eq. (A7) into Eq. (A2) and making some rearrangements, we find for the linear susceptibility in the local-field approximation

$$\chi_{\mathrm{LFA}}^{(1)}(-\omega;\omega)=\sum_n\mathbf{L}_n(\omega)\cdot\gamma_n^{(1)}(-\omega;\omega) , \tag{A8}$$

where $\mathbf{L}_n(\omega)$ is the local-field tensor:

$$\mathbf{L}_n(\omega)\equiv\sum_{\sigma,m}\frac{\boldsymbol{\mu}_m\boldsymbol{\mu}_n}{\mu_n^2}\xi_{\sigma m}(\omega)\xi_{\sigma n}^*(\omega)\frac{D_n(\omega)}{\Lambda_\sigma(\omega)} . \tag{A9}$$

$\mathbf{L}_n(\omega)$ has rank two and in Eq. (A8) its second index is contracted with the first index of the tensor $\gamma^{(1)}$. If we restrict to the RWA for the linear polarizability [Eq. (15a)], we have $D_n(\omega)=\Omega_n-\omega-i\Gamma$. It then follows immediately that the matrix $\mathbf{M}(\omega)$ is diagonalized by exactly the same transformation $\varphi_{\sigma n}$ (independent of ω) that diagonalizes the one-exciton problem in Sec. II of the main text. The eigenvalues are then $\Lambda_\sigma(\omega)=\Omega_\sigma-\omega-i\Gamma$ and we obtain for the local-field tensor

$$\mathbf{L}_n(\omega)=\sum_{\sigma,m}\frac{\boldsymbol{\mu}_m\boldsymbol{\mu}_n}{\mu_n^2}\varphi_{\sigma m}\varphi_{\sigma n}^*\frac{\omega-\Omega_n+i\Gamma}{\omega-\Omega_\sigma+i\Gamma} . \tag{A10}$$

We thus see that the local-field factor is totally determined by the solution to the one-exciton problem only. This even holds if we do not restrict our analysis to the RWA, as we will show at the end of this appendix. We also note that the LFA is exact in the case of linear optics, as follows from combining Eqs. (A8), (A10), (15a), and (10), and comparing the result with Eq. (11).

We now move to the third-order response. Comparing terms of third order in the external field that occur to the left- and right-hand sides of Eq. (19), we find

$$\sum_m M_{nm}(\omega_i)p_{ni}^{(3)}=D_n(\omega_i)\frac{\boldsymbol{\mu}_n}{\mu_n^2}\cdot\sum_{j,k,l}{}^*\gamma_n^{(3)}(-\omega_i;\omega_j,\omega_k,\omega_l)\vdots\mathbf{E}_{\mathrm{loc},j}^{(1)}(\mathbf{r}_n)\mathbf{E}_{\mathrm{loc},k}^{(1)}(\mathbf{r}_n)\mathbf{E}_{\mathrm{loc},l}^{(1)}(\mathbf{r}_n) , \tag{A11}$$

where the first-order local electric field contains the external electric field and the first-order contributions from the other dipoles (*vide infra*). The left-hand side of Eq. (A11) follows from combining the first right-hand side term of Eq. (19) with its left-hand side and describes free propagation of the third-order polarization; the right-hand side of Eq. (A11) gives the source term for the third-order polarization in terms of the first-order local fields and derives from the second right-hand side term in Eq. (19). With the notation developed above, Eq. (A11) is easily solved and the ith frequency component of the assembly's third-order dipole is obtained as

$$\mathbf{P}_i^{(3)}=\sum_n\mathbf{L}_n(\omega_i)\cdot\sum_{j,k,l}{}^*\gamma_n^{(3)}(-\omega_i;\omega_j,\omega_k,\omega_l)\vdots\mathbf{E}_{\mathrm{loc},j}^{(1)}(\mathbf{r}_n)\mathbf{E}_{\mathrm{loc},k}^{(1)}(\mathbf{r}_n)\mathbf{E}_{\mathrm{loc},l}^{(1)}(\mathbf{r}_n) . \tag{A12}$$

Finally, we have to work out the local fields:

$$\boldsymbol{\mu}_n\cdot\mathbf{E}_{\mathrm{loc},j}^{(1)}(\mathbf{r}_n)=\boldsymbol{\mu}_n\cdot\mathbf{E}_j-\sum_{m\,(\neq n)}\hbar V_{nm}p_{mj}^{(1)} . \tag{A13}$$

Using the first-order solutions Eq. (A7), substituting $V_{nm}=M_{nm}(\omega_j)-D_n(\omega_j)\delta_{nm}$, and using the fact that we know the diagonalization of the matrix $\mathbf{M}(\omega_j)$, this may be rearranged to

$$\boldsymbol{\mu}_n\cdot\mathbf{E}_{\mathrm{loc},j}^{(1)}(\mathbf{r}_n)=\boldsymbol{\mu}_n\cdot\mathbf{L}_n'(\omega_j)\cdot\mathbf{E}_j , \tag{A14}$$

where $\mathbf{L}'$ is a local-field factor defined as

$$\mathbf{L}_n'(\omega)\equiv\sum_{\sigma,m}\frac{\boldsymbol{\mu}_n\boldsymbol{\mu}_m}{\mu_n^2}\xi_{\sigma n}(\omega)\xi_{\sigma m}^*(\omega)\frac{D_n(\omega)}{\Lambda_\sigma(\omega)} . \tag{A15}$$

Note that $\mathbf{L}'$ differs from $\mathbf{L}$ [Eq. (A9)] in its tensor character and in the complex conjugation of the eigenvectors. Combining Eqs. (A12)–(A14), we find for the third-order susceptibility within the LFA

$$\chi^{(3)}_{\mathrm{LFA}}(-\omega_i;\omega_j,\omega_k,\omega_l)=\sum_n \mathbf{L}_n(\omega_i)\cdot\gamma^{(3)}_n(-\omega_i;\omega_j,\omega_k,\omega_l)\vdots\mathbf{L}'_n(\omega_j)\mathbf{L}'_n(\omega_k)\mathbf{L}'_n(\omega_l)\ . \tag{A16}$$

If ω_j is replaced by $-\omega_j$, $\mathbf{L}'_n(\omega_j)$ should be replaced by its complex conjugate (analogous for k and l). In the RWA, $\mathbf{L}'$ reduces to [cf. Eq. (A10)]

$$\mathbf{L}'_n(\omega)=\sum_{\sigma,m}\frac{\boldsymbol{\mu}_n\boldsymbol{\mu}_m}{\mu_n^2}\varphi_{\sigma n}\varphi^*_{\sigma m}\frac{\omega-\Omega_n+i\Gamma}{\omega-\Omega_\sigma+i\Gamma}\ . \tag{A17}$$

We further note that if the transition dipoles of the individual molecules are equal in magnitude and have the same orientation, the local-field tensors become simple scalars that are obtained from Eqs. (A10) and (A17) by omitting the factors $\boldsymbol{\mu}_m\boldsymbol{\mu}_n/\mu_n^2$ and $\boldsymbol{\mu}_n\boldsymbol{\mu}_m/\mu_n^2$, respectively. If, furthermore, the eigenvectors $\varphi_{\sigma m}$ are real, L and L' are equal, and we obtain Eqs. (20) and (21) in the main text.

To end this appendix, we briefly discuss the connection between the LFA and the one-exciton problem in case we do not make the RWA. It turns out that then the local-field factors are also completely determined by the one-excitons, provided that we do not apply the Heitler-London approximation in the intermolecular interaction. Relaxing the RWA, the molecular polarizability reads

$$\gamma^{(1)}_n(-\omega;\omega)=\frac{1}{\hbar}\frac{2\Omega_n\boldsymbol{\mu}_n\boldsymbol{\mu}_n}{\Omega_n^2-(\omega+i\Gamma)^2}\ . \tag{A18}$$

Furthermore, if we relax the HLA, the assembly's Hamiltonian reads [25,26]

$$\hat{H}_0=\sum_n\hbar\Omega_n\hat{B}^\dagger_n\hat{B}_n+\tfrac{1}{2}{\sum_{n,m}}'\hbar V_{nm}(\hat{B}^\dagger_n+\hat{B}_n)(\hat{B}^\dagger_m+\hat{B}_m)\ , \tag{A19}$$

which differs from Eq. (6) by the contributions proportional to $\hat{B}^\dagger_n\hat{B}^\dagger_m$ and $\hat{B}_n\hat{B}_m$ that connect states with different numbers of excitations. Therefore the name "one-excitons" should be redefined. As usual, we define them as the eigenmodes of the Hamiltonian when the exciton population in the assembly is neglected, so that Bose commutation relations apply to the operators $\hat{B}_n$ and $\hat{B}^\dagger_n$ [25,26,35]. The dispersion relation for the eigenfrequencies ω of these modes follow in a straightforward way from the coupled Heisenberg equations of motion for the operators $\hat{B}_n$ and $\hat{B}^\dagger_n$ (all n), and reads

$$\det[\mathbf{M}(\omega)]=0\ , \tag{A20}$$

where the matrix $\mathbf{M}(\omega)$ has the same form as in Eq. (A6a), with now

$$D_n(\omega)=[\Omega_n^2-(\omega+i\Gamma)^2]/2\Omega_n\ . \tag{A21}$$

We note that this form for $D_n(\omega)$ indeed coincides with the definition (A4), provided that we use the general form Eq. (A18) for the linear polarizability. We thus see that also if we do not apply the RWA, the local-field factors are fully determined by the one-exciton problem, *as long as we do not make the HLA.* We finally note that the linear susceptibility is in general (i.e., without RWA and without HLA) given by

$$\chi^{(1)}(-\omega;\omega)=\sum_{n,m,\sigma}\frac{\boldsymbol{\mu}_m\boldsymbol{\mu}_n}{\hbar\Lambda_\sigma(\omega)}\xi_{\sigma m}(\omega)\xi^*_{\sigma n}(\omega)\ . \tag{A22}$$

This follows from the above-mentioned equations of motion for $\hat{B}_n$ and $\hat{B}^\dagger_n$ in the Bose approximation in the presence of an electric field. Substituting Eqs. (A18) and (A21) into Eqs. (A8) and (A9), we observe that the exact result Eq. (A22) equals the local-field result. This proves that the linear susceptibility obtained within the LFA is always exact, irrespective of the RWA.

[1] G. Scheibe, Angew. Chem. **50**, 212 (1937); E. E. Jelley, Nature (London) **139**, 631 (1937).

[2] B. Kopainsky, J. K. Hallermeier, and W. Kaiser, Chem. Phys. Lett. **87**, 7 (1982); E. W. Knapp, P. O. J. Scherer, and S. F. Fischer, *ibid.* **111**, 481 (1984).

[3] D. V. Brumbaugh, A. A. Muenter, W. Knox, G. Mourou, and B. Wittmershaus, J. Lumin. **31/32**, 783 (1984).

[4] S. de Boer, K. J. Vink, and D. A. Wiersma, Chem. Phys. Lett. **137**, 99 (1987).

[5] J. Grad, G. Hernandez, and S. Mukamel, Phys. Rev. A **37**, 3835 (1988).

[6] V. Mizrahi, G. I. Stegeman, and W. Knoll, Phys. Rev. A **39**, 3555 (1989).

[7] R. Hirschmann and J. Friedrich, J. Chem. Phys. **91**, 7988 (1989).

[8] Y. Wang, J. Opt. Soc. Am. B **8**, 981 (1991).

[9] H. Isihara and K. Cho, Phys. Rev. B **42**, 1724 (1990).

[10] F. C. Spano and S. Mukamel, Phys. Rev. A **40**, 5783 (1989).

[11] F. C. Spano and S. Mukamel, Phys. Rev. Lett. **66**, 1197 (1991); J. Chem. Phys. **95**, 7526 (1991).

[12] H. Fidder, J. Knoester, and D. A. Wiersma, Chem. Phys. Lett. **171**, 529 (1990).

[13] H. Fidder and D. A. Wiersma, Phys. Rev. Lett. **66**, 1501 (1991).

[14] H. Fidder, J. Knoester, and D. A. Wiersma, J. Chem. Phys. **95**, 7880 (1991).

[15] J. R. G. Thorne, Y. Osaka, J. M. Zeigler, R. M. Hochstrasser, Chem. Phys. Lett. **162**, 455 (1989); A. Tilgner, H. P. Trommsdorff, J. M. Zeigler, and R. M. Hochstrasser, J. Chem. Phys. **96**, 781 (1992).

[16] C. P. DeMelo and R. Silbey, J. Chem. Phys. **88**, 2558 (1987); **88**, 2567 (1987); Z. G. Soos and G. W. Hayden, Chem. Phys. **143**, 199 (1990); S. Abe, M. Schreiber, and

W.-P. Su, Chem. Phys. Lett. **192**, 425 (1992); S. Mukamel and H. X. Wang, Phys. Rev. Lett. **69**, 65 (1992).
[17] W. B. Bosma, S. Mukamel, B. I. Greene, and S. Schmitt-Rink, Phys. Rev. Lett. **68**, 2456 (1992).
[18] E. Hanamura, Phys. Rev. B **37**, 1273 (1988); **38**, 1228 (1988).
[19] A. Nakamura, H. Yamada, and T. Tokizaki, Phys. Rev. B **40**, 8585 (1989).
[20] T. Itoh, M. Furumiya, T. Ikehara, and C. Gourdon, Solid State Commun. **73**, 271 (1990).
[21] K. Misawa, H. Yao, T. Hayashi, and T. Kobayashi, J. Chem. Phys. **94**, 4131 (1991).
[22] J. Knoester, Phys. Rev. Lett. **68**, 654 (1992).
[23] E. W. Knapp, Chem. Phys. **85**, 73 (1984).
[24] D. S. Chemla and J. Zyss, *Nonlinear Optical Properties of Organic Molecules and Crystals* (Academic, New York, 1987), Vols. I and II.
[25] A. S. Davydov, *Theory of Molecular Excitons* (Plenum, New York, 1971).
[26] V. M. Agranovich and M. D. Galanin, in *Electronic Excitation Energy Transfer in Condensed Matter,* edited by V. M. Agranovich and A. A. Maradudin (North-Holland, Amsterdam, 1982).
[27] N. Bloembergen, *Nonlinear Optics* (Benjamin, New York, 1965).
[28] Y. R. Shen, *The Principles of Nonlinear Optics* (Wiley, New York, 1984).
[29] J. Knoester and S. Mukamel, Phys. Rev. A **41**, 3812 (1990).
[30] C. J. F. Böttcher, *Theory of Electric Polarisation* (Elsevier, New York, 1952).
[31] G. Cnossen, K. E. Drabe, and D. A. Wiersma, J. Chem. Phys. **97**, 4512 (1992).
[32] F. C. Spano, J. Chem. Phys. **96**, 8109 (1992).
[33] P. W. Anderson, Phys. Rev. **109**, 1492 (1958).
[34] S. Mukamel and R. F. Loring, J. Opt. Soc. Am. B **3**, 595 (1986).
[35] J. Knoester and S. Mukamel, Phys. Rep. **205**, 1 (1991).
[36] R. H. Lehmberg, Phys. Rev. A **2**, 883 (1970).
[37] R. W. Boyd and S. Mukamel, Phys. Rev. A **29**, 1973 (1984).
[38] F. C. Spano, Phys. Rev. Lett. **67**, 3424 (1991); **68**, 2976 (1992).
[39] S. Mukamel, Z. Deng, and J. Grad, J. Opt. Soc. Am. B **5**, 804 (1988).
[40] E. Lieb, T. Schultz, and D. Mattis, Ann. Phys. (N.Y.) **16**, 407 (1961).
[41] D. B. Chesnut and A. Suna, J. Chem. Phys. **39**, 146 (1963).
[42] The difference between the one-exciton terms ($\chi_1^{(3)}$) in Eq. (28) and Eq. (9) of Ref. [38] is negligible if the separation between the various one-exciton levels is large compared to Γ. In general, Eq. (28) is the correct form. The overall factor of 2 difference with Ref. [38] derives from the factor $\frac{1}{2}$ in the right-hand side of Eq. (3).
[43] NAG FORTRAN Library Manual (Mark 14), Numerical Algorithms Group (1989) (unpublished).
[44] M. Schreiber and Y. Toyozawa, J. Phys. Soc. Jpn. **51**, 1528 (1981); **51**, 1537 (1981).
[45] J. Knoester, Chem. Phys. Lett. **203**, 371 (1993).